mathematics

MDPI

Article

Knacks of Fractional Order Swarming Intelligence for Parameter Estimation of Harmonics in Electrical Systems

Naveed Ahmed Malik [1], Ching-Lung Chang [2], Naveed Ishtiaq Chaudhary [3,*], Muhammad Asif Zahoor Raja [3], Khalid Mehmood Cheema [4], Chi-Min Shu [5] and Sultan S. Alshamrani [6]

1 Graduate School of Engineering Science and Technology, National Yunlin University of Science and Technology, 123 University Road, Section 3, Douliou, Yunlin 64002, Taiwan; d10910223@yuntech.edu.tw
2 Department of Computer Science and Information Engineering, National Yunlin University of Science and Technology, 123 University Road, Section 3, Douliou, Yunlin 64002, Taiwan; chang@yuntech.edu.tw
3 Future Technology Research Center, National Yunlin University of Science and Technology, 123 University Road, Section 3, Douliou, Yunlin 64002, Taiwan; rajamaz@yuntech.edu.tw
4 Department of Electronic Engineering, Fatima Jinnah Women University, Rawalpindi 46000, Pakistan; khalid.mehmood@fjwu.edu.pk
5 Department of Safety, Health, and Environmental Engineering, National Yunlin University of Science and Technology, 123 University Road, Section 3, Douliou, Yunlin 64002, Taiwan; shucm@yuntech.edu.tw
6 Department of Information Technology, College of Computer and Information Technology, Taif University, Taif 21944, Saudi Arabia; susamash@tu.edu.sa
* Correspondence: chaudni@yuntech.edu.tw

Citation: Malik, N.A.; Chang, C.-L.; Chaudhary, N.I.; Raja, M.A.Z.; Cheema, K.M.; Shu, C.-M.; Alshamrani, S.S. Knacks of Fractional Order Swarming Intelligence for Parameter Estimation of Harmonics in Electrical Systems. *Mathematics* **2022**, *10*, 1570. https://doi.org/10.3390/math10091570

Academic Editor: Jing Chen

Received: 1 April 2022
Accepted: 3 May 2022
Published: 6 May 2022

Abstract: The efficient parameter estimation of harmonics is required to effectively design filters to mitigate their adverse effects on the power quality of electrical systems. In this study, a fractional order swarming optimization technique is proposed for the parameter estimation of harmonics normally present in industrial loads. The proposed fractional order particle swarm optimization (FOPSO) effectively estimates the amplitude and phase parameters corresponding to the first, third, fifth, seventh and eleventh harmonics. The performance of the FOPSO was evaluated for ten fractional orders with noiseless and noisy scenarios. The robustness efficiency of the proposed FOPSO was analyzed by considering different levels of additive white Gaussian noise in the harmonic signal. Monte Carlo simulations confirmed the reliability of the FOPSO for a lower fractional order ($\lambda = 0.1$) with a faster convergence rate and no divergent run compared to other fractional orders as well as to standard PSO ($\lambda = 1$).

Keywords: fractional calculus; harmonics; parameter estimation; swarm optimization; systems

MSC: 26A33; 97M50

1. Introduction

Parameter estimation is an essential or fundamental step in solving various engineering and applied sciences problems [1–4] including monitoring power quality and assessing reliability in electrical systems [5]. Parameter estimation of electrical harmonics is required to compensate or mitigate their adverse effects in electrical systems that may lead to reduced lifetime of complex/sensitive equipment due to circuit breaker failure, enhanced core losses in electrical devices/components, instrumentation malfunctioning and excessive heat generation [6–8]. Researchers have proposed various local/global search parameter estimation methods to address the power systems harmonics issue. For instance, Singh et al. presented a Kalman filtering approach [9], Joorabian et al. proposed a novel method by hybridizing least squares with Adaline [10], Enayati et al. designed a hybrid algorithm integrating recursive least squares with an iterated Kalman filter [11], Sarkar et al. introduced a self-organized ADALINE mechanism [12], Liu et al. presented a hierarchical iterative estimation approach [13], and Xu et al. proposed various modifications in least squares and gradient descent algorithms in [14,15], and references cited therein, for the parameter estimation of power signals.

The efficacy of evolutionary and swarm optimization techniques is well-established in the literature for solving different optimization and estimation problems [16–18]. The researchers exploited their renowned strength to estimate the parameters of harmonics in electrical systems. Some of the relevant examples are as follows: Ray et al. proposed a bacterial foraging optimization technique [19], Mehmood et al. exploited differential evolution and backtracking search algorithms [20,21], Elvira-Ortiz et al. presented a genetic algorithm approach [22], Nascimento Sepulchro et al. introduced an evolutionary strategy [23], Subramaniyan et al. developed an improved football game optimization approach [24], Singh at al. designed a hybrid firefly algorithm [25], and Kabalci et al. introduced an artificial bee colony mechanism [26].

In the last decade, a new concept of designing fractional order algorithms has emerged [27,28]. Fractional order algorithms have been developed by exploiting the theories and concepts of fractional calculus in conventional algorithms. Fractional calculus generalizes the standard integer calculus to real values and provides better modeling and insight to the system under study due to promising features that include history information or the long memory principle [29–31]. Fractional order approaches are exploited to effectively solve different problems. Examples include the following: Khan et al. developed fractional order gradient algorithms for recommender systems [32,33], Yousri et al. designed fractional cuckoo search, fractional flower pollination and fractional modified Harris Hawks optimization algorithms for different applications [34–36], Chaudhary and Zubair et al. proposed fractional least-mean-squares-based methods for the parameter estimation of power signals [37–39], Machado et al. introduced the concept of particle swarm optimization (PSO) with fractional velocity [40]. and Couceiro et al. introduced the concept of a fractional order Darwinian PSO [41,42]. Later, different fractional order variants of PSO were introduced for diverse applications [43–45] including power and electrical engineering [46,47]. These successful applications of the fractional order PSO techniques motivated the authors to investigate exploiting the fractional order swarming optimization paradigm for efficient parameter estimation of harmonics in electrical systems.

The contributions of the current study are summarized as:

- A fractional order swarming optimization approach exploiting the inherited legacy of the fractional calculus is presented for the nonlinear parameter estimation problem of electrical harmonics.
- The proposed fractional order particle swarm optimization (FOPSO) effectively estimates the amplitude and phase parameters of the harmonic signal compared with the standard counterpart for different scenarios of additive white Gaussian noise.
- The best convergence performance of the FOPSO is obtained for a fractional order of 0.1 that reduces gradually with increase in the fractional order until unity (standard PSO).
- The reliability analyses, through autonomous executions of the FOPSO for harmonics parameter identification, confirm superior performance in the case of a fractional order of 0.1 for all noise variations.

The remaining article is structured as follows: A mathematical model for harmonics estimation is provided in Section 2. The proposed methodology for the problem is presented in Section 3. Simulation results, in terms of different tabular and graphical illustrations, are provided in Section 4. The conclusions of the study are provided in Section 5.

2. Harmonics Identification Model

Mathematically, the electrical harmonic signal, in terms of the amplitude, frequency and phase parameters signal, can be written as [13,14]:

$$s(t) = \sum_{k=1}^{K} \alpha_k \sin(\beta_k t + \gamma_k) + \delta(t), \tag{1}$$

where K is order of the harmonic, β_k denotes the angular frequency of the kth harmonic, defined as $\beta_k = k2\pi f_0$ with f_0 as fundamental frequency, α_k and γ_k are the amplitude and phase corresponding to the kth harmonic, while δ is used to represent additive white Gaussian noise. Writing Equation (1) in discrete form by sampling the signal $s(t)$ with period l, then $t_m = ml$

$$s[t_m] = \sum_{k=1}^{K} \alpha_k \sin[\beta_k t_m + \gamma_k] + \delta[t_m]. \tag{2}$$

For simplicity, assume $s(t_m) = s(m)$ and rewriting (2) as

$$s[m] = \sum_{k=1}^{K} \alpha_k \sin[\beta_k m + \gamma_k] + \delta[t_m]. \tag{3}$$

Applying the trigonometric identity to (2) and expressing this in terms of the combination of cosine and sine forms

$$s[m] = \sum_{k=1}^{K} [\alpha_k \sin[\beta_k m] \cos \gamma_k + \alpha_k \cos[\beta_k m] \sin \gamma_k] + \delta[m], \tag{4}$$

assuming $x_k = \alpha_k \cos \gamma_k$ and $y_k = \alpha_k \sin \gamma_k$. Then, rewriting (4) in simplified form as

$$s[m] = \sum_{k=1}^{K} [x_k \sin[\beta_k m] + y_k \cos[\beta_k m]] + \delta[m]. \tag{5}$$

Equation (5) in terms of the identification model is expressed as

$$s[m] = \mathbf{h}^T[m]\mathbf{p} + \delta[m]. \tag{6}$$

where

$$\mathbf{h}[m] = [\sin[\beta_1 m], \cos[\beta_1 m], \sin[\beta_2 m], \cos[\beta_2 m], \ldots, \sin[\beta_k m], \cos[\beta_k m]]. \tag{7}$$

and

$$\mathbf{p} = [x_1, y_1, x_2, y_2, \ldots, x_k, y_k]. \tag{8}$$

The objective is to estimate the parameters of the harmonics by minimizing the difference between the actual harmonic signal $s[m]$ and the estimated harmonic signal $\hat{s}[m]$ through the proposed fractional order swarming optimization approach. Thus, defining the cost/objective function as

$$\varepsilon[m] = \text{mean}[s[m] - \hat{s}[m]]^2 = \left[s[m] - \mathbf{h}^T[m]\hat{\mathbf{p}}\right]^2, \tag{9}$$

since the identification model presented in Equation (6) and the cost function given in Equation (9) considers the intermediate variable as parameters to be identified, it is necessary to use the expressions relating the intermediate variables of (8) with the actual parameters of the harmonics signal (3). The required relations are given as

$$\alpha_k = \sqrt{(x_k)^2 + (y_k)^2}, \quad \gamma_k = \tan^{-1} \frac{y_k}{x_k}, \tag{10}$$

3. Methodology

The methodology for the fractional swarming optimization approach for the harmonic identification model is described concisely in terms of mathematical development, process flow illustrations and pseudocodes. An overview of the methodology in terms of fundamental block structures is presented in Figure 1.

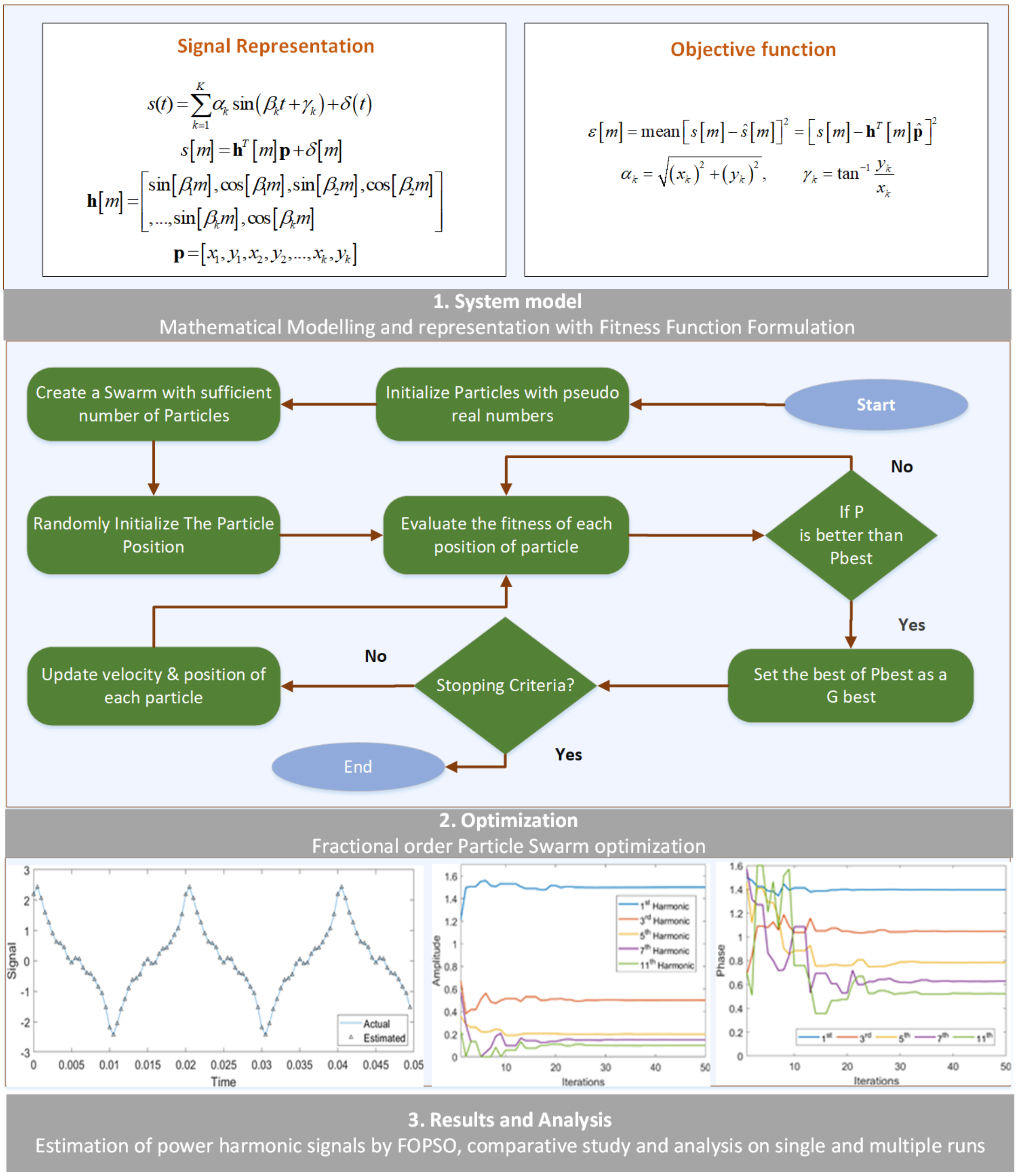

Figure 1. Graphical abstract of the proposed study exploiting FOPSO for solving the harmonic identification model.

Optimization Procedure: Fractional Swarming Computing Paradigm

A heuristic computing strategy represented with fractional order particle swarm optimization (FOPSO) was first presented by Machado with a team of researchers by introducing the fractional order velocity in the standard PSO [40]. Since its introduction, the FOPSO has been extensively used by the research community for various optimization tasks with performance better than that in integer counterparts [41–44]

The FOPSO is designed by introducing the definition of the fractional order velocity in standard PSO and the definition of the fractional derivative is given in a variety of ways, such as Grünwald–Letnikov (GL), Riemann–Liouville, Weyl, Marchaud, Caputo, Hadamard, Davidson–Essex and many others [48,49]. The similarity of all these definitions is well-established for some of their own functions and they have their own significance for different applications; however, the mathematical expressions for FOPSO with a fractional velocity are derived by implementing the GL definition for the fractional order λ, i.e., D^{λ} of signal $s(t)$ using the concept of a Euler gamma function Γ, as [50]:

$$D^{\lambda}[s(t)] = \lim_{h \to 0}\left[\frac{1}{h^{\lambda}}\sum_{k=0}^{\infty}\frac{(-1)^{k}\Gamma(\lambda+1)s(t-kh)}{\Gamma(k+1)\Gamma(\lambda-k+1)}\right], \tag{11}$$

where h is the incremental step size and the Euler gamma function is defined as, $\Gamma(z) = \int_{0}^{\infty} e^{-t}t^{z-1}$.

The finite time representation of Equation (11) can be given as follows:

$$D^{\lambda}[s(t)] = \frac{1}{T^{\lambda}}\sum_{k=0}^{kr}\frac{(-1)^{k}\Gamma(\lambda+1)s(t-kT)}{\Gamma(k+1)\Gamma(\lambda-k+1)}, \tag{12}$$

where Kr represents the order of truncation and T denotes the sampling period. Before proceeding regarding how Equations (11) and (12) are used to derive FOPSO, first, we introduce the mathematical expressions for the velocity v and position x of traditional PSO in the case of the nth particle as follows:

$$v^{n}(j+1) = \omega v^{n}(j) + \rho_1 r_1 (Lb^{n}(j) - x^{n}(j)) + \rho_2 r_2 (Gb^{n}(j) - x^{n}(j)), \tag{13}$$

$$x^{n}(j+1) = x^{n}(j) + v^{n}(j+1), \tag{14}$$

where j is used to represent the flight index, ω stands for the inertia weight, Lb is a local best particle, Gb is the representation for the global best particle, ρ_1 and ρ_2 are cognitive and social acceleration parameters, respectively, while r_1 and r_2 are the pseudo-random values taken between 0 and 1.

By assuming $\omega = 1$ in (13), while $T = 1$, $s(t) = v^{n}(t)$ and replacing j by $j + 1$ in (12), one may obtain the mathematical relation of the fractional velocity in FOPSO as follows [50]:

$$\begin{aligned} v^{n}(j+1) = {} & -\sum_{k=1}^{kr}\frac{(-1)^{k}\Gamma(\lambda+1)v^{n}(j+1-k)}{\Gamma(k+1)\Gamma(\lambda-k+1)} + \\ & \rho_1 r_1 (Lb^{n}(j) - x^{n}(j)) + \rho_2 r_2 (Gb^{n}(j) - x^{n}(j)) \end{aligned} \tag{15}$$

The fractional velocity representation of FOPSO for n^{th} particle with k^{th} term, i.e., $kr = 1, 2, \ldots, k$, as:

$$\begin{aligned} v^{n}(j+1) = {} & \lambda v^{n}(j) + \tfrac{1}{2}\lambda(1-\lambda)v^{n}(j-1) + \cdots \\ & + \tfrac{1}{\Gamma(k+1)}(\lambda(1-\lambda)(2-\lambda)\cdots(k-1-\lambda))v^{n}(j-k+1) \\ & + \rho_1 r_1 (Lb^{n}(j) - x^{n}(j)) + \rho_2 r_2 (Gb^{n}(j) - x^{n}(j)) \end{aligned} \tag{16}$$

The velocity update Equation (16) and position update Equation (14) formulate the FOPSO. Further details regarding the FOPSO can be found in [50].

For implementation of the FOPSO for the harmonic identification model, the workflow procedure of methodology is shown in Figure 1, the genetic flow diagram of the FOPSO in the form of procedural steps is given in Figure 2, while the performance of cognitive and social learning behavior of FOPSO is illustrated in Figure 3. The pseudocode of the FOPSO for the harmonic identification model is provided in Algorithm 1. The velocity update equation of FOPSO for $Kr = 4$ is used as given below:

$$\begin{aligned} v^n(j+1) = \; & \lambda v^n(j) + \tfrac{1}{2}\lambda(1-\lambda)v^n(j-1) + \cdots \\ & + \tfrac{1}{24}(\lambda(1-\lambda)(2-\lambda)\cdots(3-\lambda))v^n(j-3) \\ & + \rho_1 r_1 (Lb^n(j) - x^n(j)) + \rho_2 r_2 (Gb^n(j) - x^n(j)), \end{aligned} \tag{17}$$

and the position update is given as

$$x^n(j+1) = x^n(j) + v^n(j+1) \tag{18}$$

The parameter settings for implementation of the FOPSO were adopted through experience and much experimentation. All the parameters were set after conducting exhaustive experiments since small variations in these settings can result in premature convergence and/or some time divergence. The parameter settings are given as follows: eight decision variables for the optimization problem were set, i.e., particle size = 8, swarm size = 250 particles, flights or iterations = 100, cognitive and global acceleration factors = 2, inertia weight = 0.97, λ, maximum/minimum velocities = [0.4, -0.4], and fractional order λ = [0.1, 0.2, ... , 1]. The computer simulations for FOPSO were performed in the MATLAB software package in a Windows 10 environment.

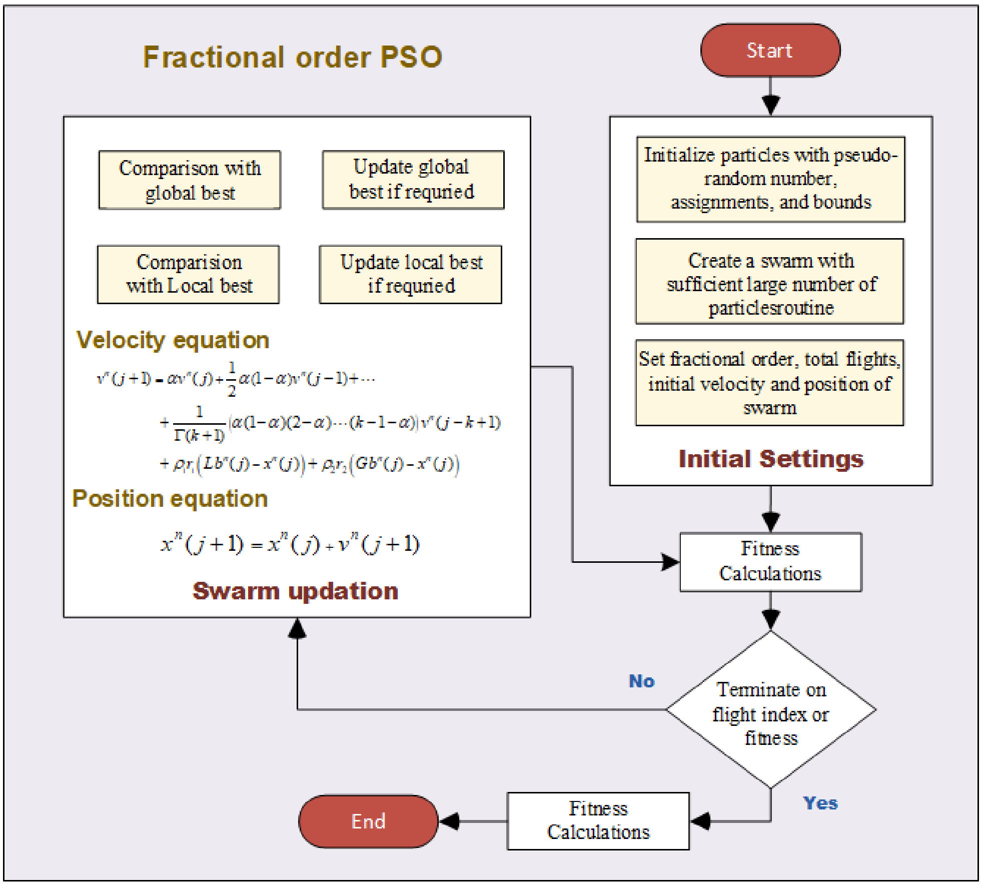

Figure 2. Process flow diagram of the FOPSO.

Algorithm 1. Pseudocode for FOPSO to solve the harmonics identification model

Inputs: Create particle $\boldsymbol{p}$ with elements equivalent to number of unknown parameters in the signal $s(t)$ as

$$\boldsymbol{p} = [\,\boldsymbol{\alpha} \quad \boldsymbol{\gamma}\,] = [\,(\alpha_1, \alpha_2, \ldots, \alpha_{n_a}) \quad (\gamma_1, \gamma_2, \ldots, \gamma_{n_\gamma})\,],$$

and set of P formulate a swarm.

$$\text{Swarm position } \boldsymbol{X} = \begin{bmatrix} \boldsymbol{x}_1 \\ \boldsymbol{x}_2 \\ \vdots \\ \boldsymbol{x}_m \end{bmatrix} = \begin{bmatrix} (\alpha_{1,1}, \alpha_{2,1}, \ldots, \alpha_{n_a,1}) & (\gamma_{1,1}, \gamma_{2,1}, \ldots, \gamma_{n,1}) \\ (\alpha_{1,1}, \alpha_{2,1}, \ldots, \alpha_{n_a,1}) & (\gamma_{1,1}, \gamma_{2,1}, \ldots, \gamma_{n,1}) \\ \vdots & \vdots \\ (\alpha_{1,1}, \alpha_{2,1}, \ldots, \alpha_{n_a,1}) & (\gamma_{1,1}, \gamma_{2,1}, \ldots, \gamma_{n,1}) \end{bmatrix},$$

for m number of $\boldsymbol{p} = \boldsymbol{x}$ in $\boldsymbol{X}$. The associated velocity $\boldsymbol{V}$ with position is created similarly.

Output: The particle $\boldsymbol{x}$ of FOPSO with best fitness as defined in (9)

Start FOPSO

Step 1: ***Initialization:*** Bound pseudo-real numbers are randomly generated to form an initial swarm X with m number of particles x. Accordingly, associate the initialize velocities v to each particle. Set the values of decision variables, i.e., particle size, swarm size, flights or iterations, cognitive and global acceleration factors, inertia weight, maximum and minimum velocities, and fractional order

Step 2: ***Fitness evaluation***: Determine the fitness of each particle $\boldsymbol{x}$ of $\boldsymbol{X}$ using Equation (9).

Step 3: ***Termination***: Stop the execution of FOPSO for fulfilment of any of the following:

(a) Total number of flights/iterations are executed
(b) Tolerance limits are attained, i.e., via calculation of the difference between present and previous local/global best particles

If termination conditions are fulfilled then proceed from step 5, otherwise continue

Step 4: ***Updating mechanism***: The velocity and position of FOPSO algorithms, as defined in Equaitons (14) and (16), respectively, are updated on each flight taking into consideration the local/global best particle $\boldsymbol{x}$ of the swarm $\boldsymbol{X}$.
Go to Step 2 with updated swarm $\boldsymbol{X}$.

Step 5: **Analysis of fractional order:** Repeat steps 1 to 4 by varying the fractional order α of the velocity in the FOPSO algorithms.

Step 6: **Storage**: Store the values of the parameter for global best particle $\boldsymbol{x}$, align the fitness, execution time for the current run of FOPSO with different fractional orders.

Step 7: **Replication:** Conduct repetition of steps 1 to 6 for the harmonic identification model with small as well as large signal-to-noise ratios.

Step 8: **Statistics:** Create a resaonable dataset by repetition of the FOPSO algorithm from step 1 to 7 for multiple trials to perform a reliable and exhaustive statistical analysis.

End FOPSO

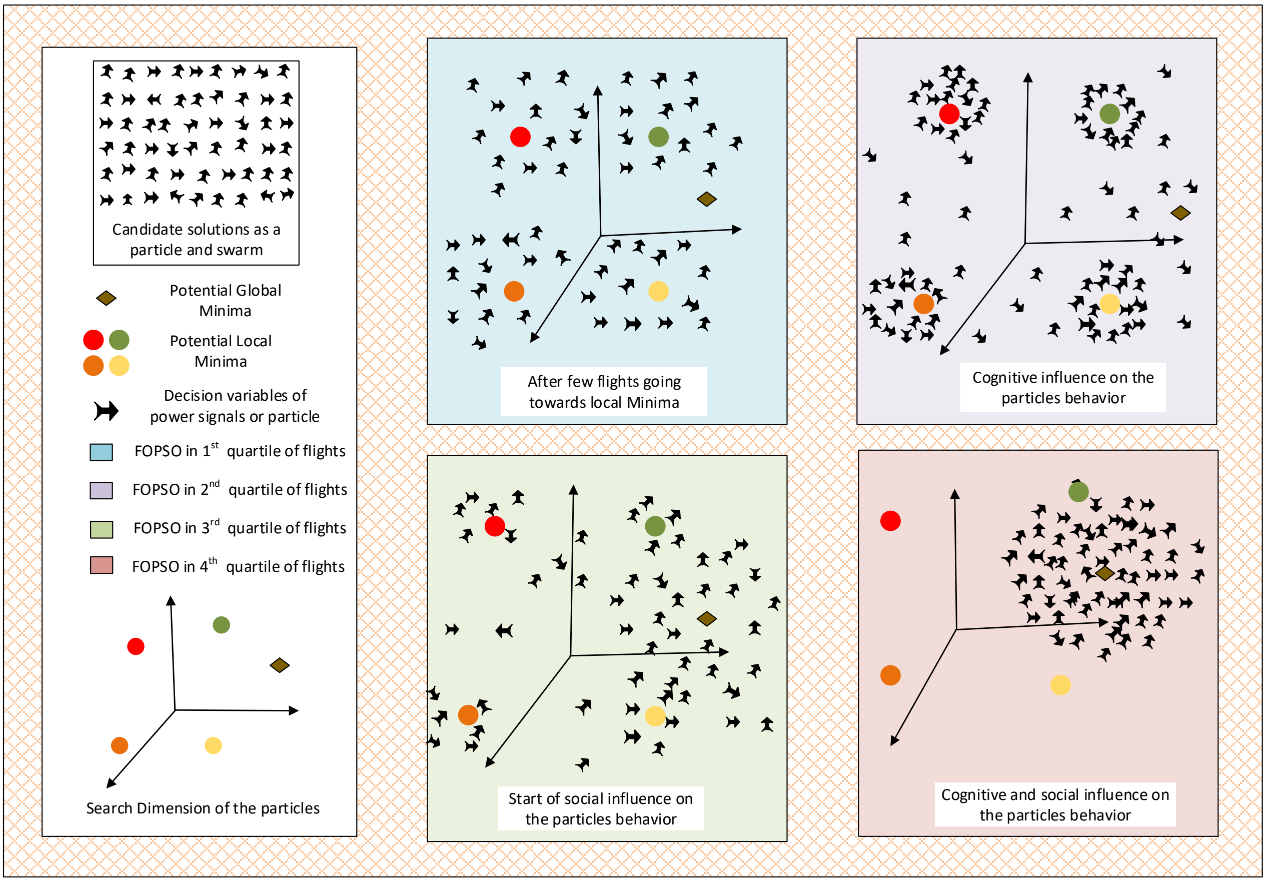

Figure 3. Generic diagram for working principle of FOPSO.

4. Results and Discussion

In this section, numerical experimentation for power systems harmonics estimation was conducted through FOPSO and the results are presented in tabular/graphical illustrations, along with necessary discussion. The estimation was not real-time and the measurement data needed to be provided before the estimation. The following example representing the harmonics signal normally present in industrial loads was considered [25,26].

$$s(t) = \begin{bmatrix} 1.5\sin(2\pi f_1 t + 1.396) + 0.5\sin(2\pi f_3 t + 1.047) + \\ 0.2\sin(2\pi f_5 t + 0.785) + 0.15\sin(2\pi f_7 t + 0.628) + \\ 0.1\sin(2\pi f_{11} t + 0.523) \end{bmatrix}. \tag{19}$$

The parameters of the harmonics signal to be estimated were

$$\begin{bmatrix} (\alpha_1, \alpha_2, \alpha_3, \alpha_4, \alpha_5) \\ (\gamma_1, \gamma_2, \gamma_3, \gamma_4, \gamma_5) \end{bmatrix} = \begin{bmatrix} 1.50, 0.50, 0.20, 0.15, 0.10 \\ 1.396, 1.047, 0.785, 0.628, 0.523 \end{bmatrix}. \tag{20}$$

The actual harmonic signal $s(t)$ in (19) was generated in Matlab, and was sampled at a 2 kHz sampling frequency. In (19), f_1 = 50, f_3 = 150, f_5 = 250, f_7 = 350, f_{11} = 550 and additive white Gaussian noise δ with 200 dB, 70 dB and 50 dB levels were added to assess the robustness of the proposed FOPSO scheme. The FOPSO was deeply analyzed for the harmonics estimation problem by considering ten fractional orders λ, ranging from 0.1 to 1, i.e., $\lambda = [0.1, 0.2, 0.3, 0.4, 0.5, 0.6, 0.7, 0.8, 0.9, 1.0]$.

The graphs of iterative learning of the FOPSO for harmonics estimation are presented in Figure 4 for $\lambda = [0.2, 0.4, 0.6, 0.8, 1.0]$. Figure 4a provides the plots for $\delta = 200$ dB, while Figure 4b,c gives the graphs for $\delta = 70$ dB and, $\delta = 50$ dB respectively. The convergence speed was faster for lower λ and decreased gradually with increasing λ, as seen in Figure 4.

In order to assess the accuracy of the parameter estimates, the results of the obtained parameters through FOPSO at different iterations are presented in Tables 1–3 for λ = 0.1, 0.5 and 1.0, respectively. The final fitness values for the case of λ = 0.1 were 8.99×10^{-21}, 5.46×10^{-8} and 5.80×10^{-6} for δ = 200 dB, 70 dB and 50 dB, respectively. While the respective values for the case of λ = 0.5 and λ = 1.0 were 8.05×10^{-21}, 4.89×10^{-8} and 6.01×10^{-6}, and 2.99×10^{-17}, 5.63×10^{-8} and 5.62×10^{-6}, respectively. The parameter estimates results for the remaining fractional orders, λ = 0.2, 0.3, 0.4, 0.6, 0.7, 0.8 and 0.9 are provided in Supplementary Tables S1–S7 in the Supplementary Material. The results indicated that the FOPSO was accurate and convergent in estimating the parameters of the power system harmonics for all λ and δ, with decrease in the precision of the estimates as the noise δ increased.

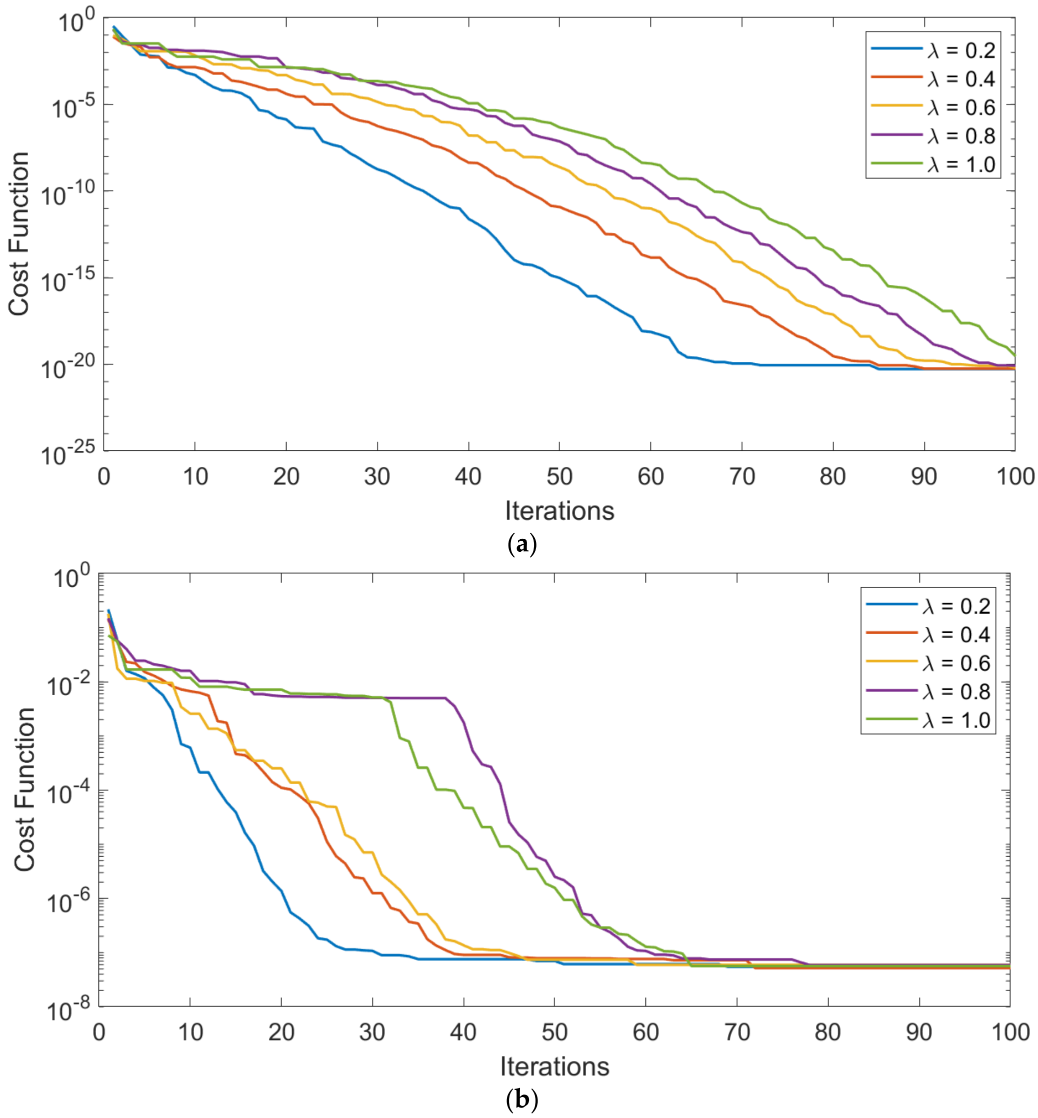

Figure 4. *Cont.*

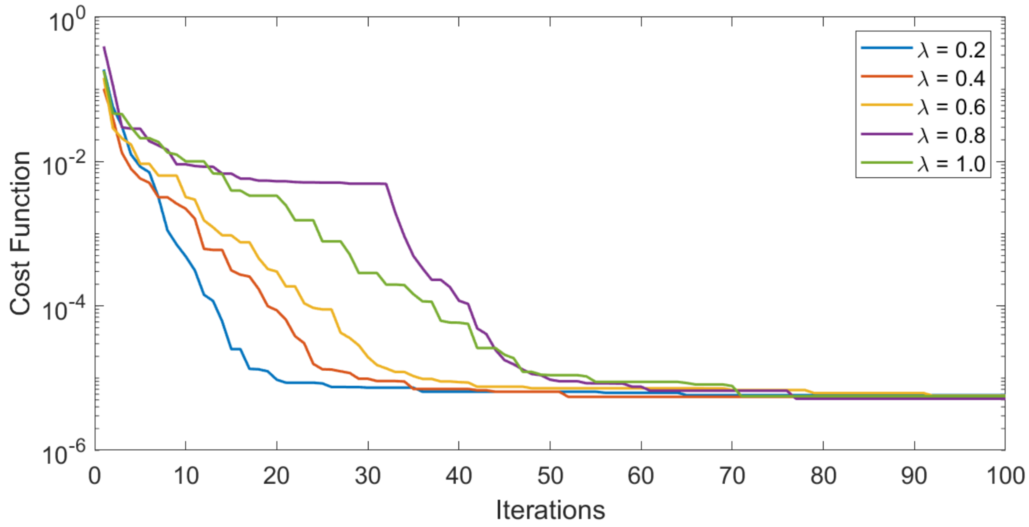

(**c**)

Figure 4. Cost function iterative adaptation for different noise scenarios. (**a**) 200 dB (**b**) 70 dB (**c**) 50 dB.

Table 1. Fitness results along with the estimated values for λ = 0.1.

δ	t	α_1	α_2	α_3	α_4	α_5	γ_1	γ_2	γ_3	γ_4	γ_5	ε
200	10	1.3877	0.4372	0.3642	0.3479	0.3401	1.5774	1.2000	1.4482	1.2608	0.4896	1.32×10^{-1}
	20	1.4907	0.4986	0.2045	0.1439	0.1062	1.3967	1.0491	0.7894	0.6153	0.5417	9.76×10^{-5}
	30	1.5000	0.5001	0.1998	0.1499	0.0998	1.3962	1.0466	0.7853	0.6287	0.5228	1.24×10^{-7}
	40	1.5000	0.5000	0.2000	0.1500	0.1000	1.3960	1.0470	0.7850	0.6280	0.5229	1.12×10^{-10}
	50	1.5000	0.5000	0.2000	0.1500	0.1000	1.3960	1.0470	0.7850	0.6280	0.5230	2.51×10^{-13}
	60	1.5000	0.5000	0.2000	0.1500	0.1000	1.3960	1.0470	0.7850	0.6280	0.5230	7.46×10^{-17}
	70	1.5000	0.5000	0.2000	0.1500	0.1000	1.3960	1.0470	0.7850	0.6280	0.5230	8.40×10^{-20}
	80	1.5000	0.5000	0.2000	0.1500	0.1000	1.3960	1.0470	0.7850	0.6280	0.5230	8.05×10^{-21}
	90	1.5000	0.5000	0.2000	0.1500	0.1000	1.3960	1.0470	0.7850	0.6280	0.5230	7.90×10^{-21}
	100	1.5000	0.5000	0.2000	0.1500	0.1000	1.3960	1.0470	0.7850	0.6280	0.5230	6.43×10^{-21}
70	10	1.2489	0.7684	0.1411	0.1246	0.3677	0.9979	0.6191	1.3253	1.2996	1.1829	3.02×10^{-1}
	20	1.4961	0.5006	0.1952	0.1432	0.1041	1.3980	1.0495	0.8365	0.6433	0.5207	1.11×10^{-4}
	30	1.5000	0.5001	0.1997	0.1500	0.1000	1.3960	1.0470	0.7860	0.6279	0.5258	1.75×10^{-7}
	40	1.4999	0.5001	0.1998	0.1501	0.1001	1.3960	1.0471	0.7849	0.6278	0.5238	9.86×10^{-8}
	50	1.4999	0.5000	0.1999	0.1500	0.1000	1.3960	1.0470	0.7850	0.6277	0.5236	7.05×10^{-8}
	60	1.4999	0.5000	0.1999	0.1500	0.1000	1.3960	1.0470	0.7850	0.6277	0.5236	7.05×10^{-8}
	70	1.4999	0.5000	0.1999	0.1500	0.1000	1.3960	1.0471	0.7850	0.6277	0.5236	6.76×10^{-8}
	80	1.4999	0.5000	0.1999	0.1500	0.1000	1.3960	1.0471	0.7850	0.6277	0.5236	6.76×10^{-8}
	90	1.5000	0.5000	0.1999	0.1500	0.1000	1.3960	1.0470	0.7850	0.6277	0.5235	5.45×10^{-8}
	100	1.5000	0.5000	0.1999	0.1500	0.1000	1.3960	1.0470	0.7850	0.6277	0.5235	5.45×10^{-8}
50	10	1.4930	0.8742	0.1745	0.2108	0.3877	1.2681	0.9908	1.1505	1.4367	0.9066	1.47×10^{-1}
	20	1.4996	0.5051	0.2012	0.1467	0.1043	1.3972	1.0443	0.7541	0.6253	0.5286	5.76×10^{-5}
	30	1.5002	0.5000	0.1993	0.1505	0.0999	1.3958	1.0477	0.7860	0.6285	0.5187	6.83×10^{-6}
	40	1.5003	0.5000	0.1992	0.1505	0.0999	1.3963	1.0477	0.7860	0.6282	0.5187	6.33×10^{-6}
	50	1.5003	0.5000	0.1992	0.1505	0.0999	1.3963	1.0477	0.7860	0.6282	0.5187	6.33×10^{-6}
	60	1.5003	0.5000	0.1992	0.1505	0.0999	1.3963	1.0477	0.7860	0.6282	0.5187	6.33×10^{-6}
	70	1.5003	0.5000	0.1992	0.1505	0.0999	1.3963	1.0477	0.7860	0.6282	0.5187	6.33×10^{-6}
	80	1.5003	0.5000	0.1992	0.1501	0.0999	1.3963	1.0480	0.7859	0.6275	0.5168	4.64×10^{-6}
	90	1.5003	0.5000	0.1992	0.1501	0.0999	1.3963	1.0480	0.7859	0.6275	0.5168	4.64×10^{-6}
	100	1.5003	0.5000	0.1992	0.1501	0.0999	1.3963	1.0480	0.7859	0.6275	0.5168	4.64×10^{-6}
		1.5000	0.5000	0.2000	0.1500	0.1000	1.3960	1.0470	0.7850	0.6280	0.5230	0

Table 2. Fitness results along with the estimated values for λ = 0.5.

δ	t	α_1	α_2	α_3	α_4	α_5	γ_1	γ_2	γ_3	γ_4	γ_5	ε
200	10	1.7149	0.8193	0.2604	0.3166	0.0804	1.1801	0.9806	0.9897	1.1337	0.7780	1.58×10^{-1}
	20	1.4966	0.4795	0.1939	0.1439	0.0000	1.3913	0.9986	0.7302	0.6952	0.5229	5.67×10^{-3}
	30	1.5018	0.4988	0.2040	0.1509	0.1030	1.3982	1.0404	0.7921	0.6052	0.5065	3.39×10^{-5}
	40	1.5001	0.5003	0.2004	0.1502	0.1003	1.3961	1.0477	0.7860	0.6303	0.5165	5.68×10^{-7}
	50	1.5000	0.4999	0.2000	0.1500	0.0999	1.3960	1.0471	0.7845	0.6277	0.5226	1.43×10^{-8}
	60	1.5000	0.5000	0.2000	0.1500	0.1000	1.3960	1.0470	0.7850	0.6280	0.5230	1.16×10^{-11}
	70	1.5000	0.5000	0.2000	0.1500	0.1000	1.3960	1.0470	0.7850	0.6280	0.5230	2.84×10^{-14}
	80	1.5000	0.5000	0.2000	0.1500	0.1000	1.3960	1.0470	0.7850	0.6280	0.5230	1.28×10^{-17}
	90	1.5000	0.5000	0.2000	0.1500	0.1000	1.3960	1.0470	0.7850	0.6280	0.5230	2.32×10^{-20}
	100	1.5000	0.5000	0.2000	0.1500	0.1000	1.3960	1.0470	0.7850	0.6280	0.5230	8.05×10^{-21}
70	10	1.4459	0.5354	0.2790	0.5387	0.2333	1.0436	1.2585	0.7510	1.3152	1.1649	2.52×10^{-1}
	20	1.4894	0.5209	0.2076	0.1430	0.0312	1.4307	1.0613	0.6887	0.7014	1.3438	5.31×10^{-3}
	30	1.4894	0.5037	0.1941	0.1530	0.1050	1.3910	1.0508	0.8394	0.6228	0.5125	1.84×10^{-4}
	40	1.4997	0.5004	0.1998	0.1508	0.1009	1.3955	1.0476	0.7831	0.6226	0.5192	1.69×10^{-6}
	50	1.4999	0.5001	0.2000	0.1500	0.1000	1.3961	1.0472	0.7847	0.6286	0.5233	9.23×10^{-8}
	60	1.4999	0.5000	0.2000	0.1500	0.1000	1.3960	1.0469	0.7848	0.6277	0.5231	6.43×10^{-8}
	70	1.4999	0.5000	0.2000	0.1500	0.1000	1.3960	1.0469	0.7848	0.6277	0.5231	6.18×10^{-8}
	80	1.4999	0.5000	0.2000	0.1500	0.1000	1.3960	1.0469	0.7848	0.6277	0.5231	4.89×10^{-8}
	90	1.4999	0.5000	0.2000	0.1500	0.1000	1.3960	1.0469	0.7848	0.6277	0.5231	4.89×10^{-8}
	100	1.4999	0.5000	0.2000	0.1500	0.1000	1.3960	1.0469	0.7848	0.6277	0.5231	4.89×10^{-8}
50	10	1.3047	0.6259	0.3958	0.3571	0.2654	1.4606	0.7557	1.1532	0.8701	1.2466	1.12×10^{-1}
	20	1.5127	0.4693	0.2060	0.1364	0.0201	1.3911	1.0300	0.8900	0.6272	1.8194	5.59×10^{-3}
	30	1.5050	0.5031	0.2086	0.1531	0.1055	1.4021	1.0264	0.7782	0.6881	0.4985	2.15×10^{-4}
	40	1.4993	0.5008	0.1981	0.1501	0.1000	1.3964	1.0508	0.7831	0.6198	0.5258	1.48×10^{-5}
	50	1.5006	0.4999	0.2015	0.1499	0.0996	1.3958	1.0480	0.7879	0.6253	0.5195	8.72×10^{-6}
	60	1.4996	0.5002	0.2001	0.1501	0.0996	1.3965	1.0473	0.7839	0.6175	0.5195	7.21×10^{-6}
	70	1.4996	0.5002	0.2001	0.1501	0.0996	1.3965	1.0473	0.7839	0.6175	0.5195	7.21×10^{-6}
	80	1.4996	0.5005	0.1997	0.1501	0.0998	1.3964	1.0470	0.7839	0.6302	0.5203	6.65×10^{-6}
	90	1.4996	0.5004	0.2001	0.1501	0.0998	1.3964	1.0471	0.7839	0.6302	0.5213	6.01×10^{-6}
	100	1.4996	0.5004	0.2001	0.1501	0.0998	1.3964	1.0471	0.7839	0.6302	0.5213	6.01×10^{-6}
		1.5000	0.5000	0.2000	0.1500	0.1000	1.3960	1.0470	0.7850	0.6280	0.5230	0

Table 3. Fitness results along with the estimated values for λ = 1.

δ	t	α_1	α_2	α_3	α_4	α_5	γ_1	γ_2	γ_3	γ_4	γ_5	ε
200	10	1.4720	0.3721	0.1285	0.4860	0.3704	1.6671	0.3728	0.6035	0.5516	0.1737	2.28×10^{-1}
	20	1.5674	0.4953	0.1743	0.1362	0.0507	1.4016	0.9911	0.6795	0.8966	0.9360	5.70×10^{-3}
	30	1.4885	0.5049	0.2047	0.1766	0.0768	1.4086	1.0527	0.6944	0.7198	0.7086	1.30×10^{-3}
	40	1.4919	0.5047	0.2056	0.1569	0.0956	1.3961	1.0382	0.7966	0.6743	0.6329	1.89×10^{-4}
	50	1.4993	0.5008	0.1996	0.1498	0.1008	1.3967	1.0397	0.7948	0.6177	0.5172	1.15×10^{-5}
	60	1.5001	0.5000	0.2002	0.1498	0.0996	1.3956	1.0473	0.7842	0.6292	0.5216	3.39×10^{-7}
	70	1.5000	0.5000	0.2000	0.1500	0.1000	1.3960	1.0471	0.7850	0.6279	0.5225	3.06×10^{-9}
	80	1.5000	0.5000	0.2000	0.1500	0.1000	1.3960	1.0470	0.7850	0.6280	0.5230	1.17×10^{-11}
	90	1.5000	0.5000	0.2000	0.1500	0.1000	1.3960	1.0470	0.7850	0.6280	0.5230	1.14×10^{-14}
	100	1.5000	0.5000	0.2000	0.1500	0.1000	1.3960	1.0470	0.7850	0.6280	0.5230	2.99×10^{-17}
70	10	1.2932	0.4226	0.2798	0.2903	0.1402	1.5028	0.6010	0.7288	0.6064	1.0279	7.18×10^{-2}
	20	1.5047	0.4803	0.2312	0.2018	0.0000	1.3832	1.0399	0.7084	0.8538	0.8948	8.14×10^{-3}
	30	1.5053	0.4840	0.1851	0.1331	0.0000	1.4128	1.0874	0.7003	0.5753	0.7488	6.08×10^{-3}
	40	1.5007	0.5009	0.1953	0.1508	0.0000	1.4056	1.0537	0.7632	0.6765	0.6764	5.16×10^{-3}
	50	1.5017	0.5035	0.1986	0.1537	0.1001	1.3918	1.0516	0.7845	0.6395	0.5623	4.66×10^{-5}
	60	1.5000	0.5006	0.2005	0.1505	0.1003	1.3960	1.0454	0.7843	0.6269	0.5236	9.40×10^{-7}
	70	1.5001	0.4999	0.1999	0.1501	0.0999	1.3961	1.0471	0.7846	0.6281	0.5215	1.25×10^{-7}
	80	1.5000	0.5000	0.1999	0.1501	0.0999	1.3960	1.0470	0.7847	0.6277	0.5235	5.63×10^{-8}
	90	1.5000	0.5000	0.1999	0.1501	0.0999	1.3960	1.0470	0.7847	0.6277	0.5235	5.63×10^{-8}
	100	1.5000	0.5000	0.1999	0.1501	0.0999	1.3960	1.0470	0.7847	0.6277	0.5235	5.63×10^{-8}

Table 3. *Cont.*

δ	t	α_1	α_2	α_3	α_4	α_5	γ_1	γ_2	γ_3	γ_4	γ_5	ε
50	10	1.3944	0.6793	0.3021	0.2184	0.4664	1.4693	0.4017	0.3648	0.8624	0.9475	1.81×10^{-1}
	20	1.5278	0.3971	0.2207	0.1943	0.0615	1.3839	0.9626	0.8229	0.6980	1.1946	1.01×10^{-2}
	30	1.5164	0.4768	0.1746	0.1624	0.0547	1.3931	1.0690	0.9385	0.5258	0.5986	2.48×10^{-3}
	40	1.5042	0.4994	0.1987	0.1366	0.0978	1.3983	1.0246	0.8289	0.6534	0.6263	2.86×10^{-4}
	50	1.5027	0.4948	0.1966	0.1521	0.0993	1.3954	1.0362	0.7925	0.6314	0.5302	5.65×10^{-5}
	60	1.5008	0.5022	0.1980	0.1493	0.0991	1.3962	1.0479	0.7838	0.6311	0.5326	1.10×10^{-5}
	70	1.5004	0.4992	0.1989	0.1482	0.0991	1.3963	1.0478	0.7831	0.6265	0.5328	8.87×10^{-6}
	80	1.4997	0.4998	0.2001	0.1501	0.0993	1.3965	1.0480	0.7838	0.6325	0.5262	5.62×10^{-6}
	90	1.4997	0.4998	0.2001	0.1501	0.0993	1.3965	1.0480	0.7838	0.6325	0.5262	5.62×10^{-6}
	100	1.4997	0.4998	0.2001	0.1501	0.0993	1.3965	1.0480	0.7838	0.6325	0.5262	5.62×10^{-6}
		1.5000	0.5000	0.2000	0.1500	0.1000	1.3960	1.0470	0.7850	0.6280	0.5230	0

The learning plots of the amplitude and phase parameters estimates, along with the constructed harmonic signal from the estimated parameters, are presented in Figures 5–8 for λ = 0.1, 0.4, 0.7 and 1.0, respectively, for the case of δ = 70 dB, while the respective plots for δ = 200 dB and 50 dB are provided in Supplementary Figures S1–S8, respectively, in the Supplementary Material. The results indicated that the FOPSO correctly estimated the amplitude and phase parameters of the harmonic signal and hence accurately reconstructed the actual signal through the estimated parameters.

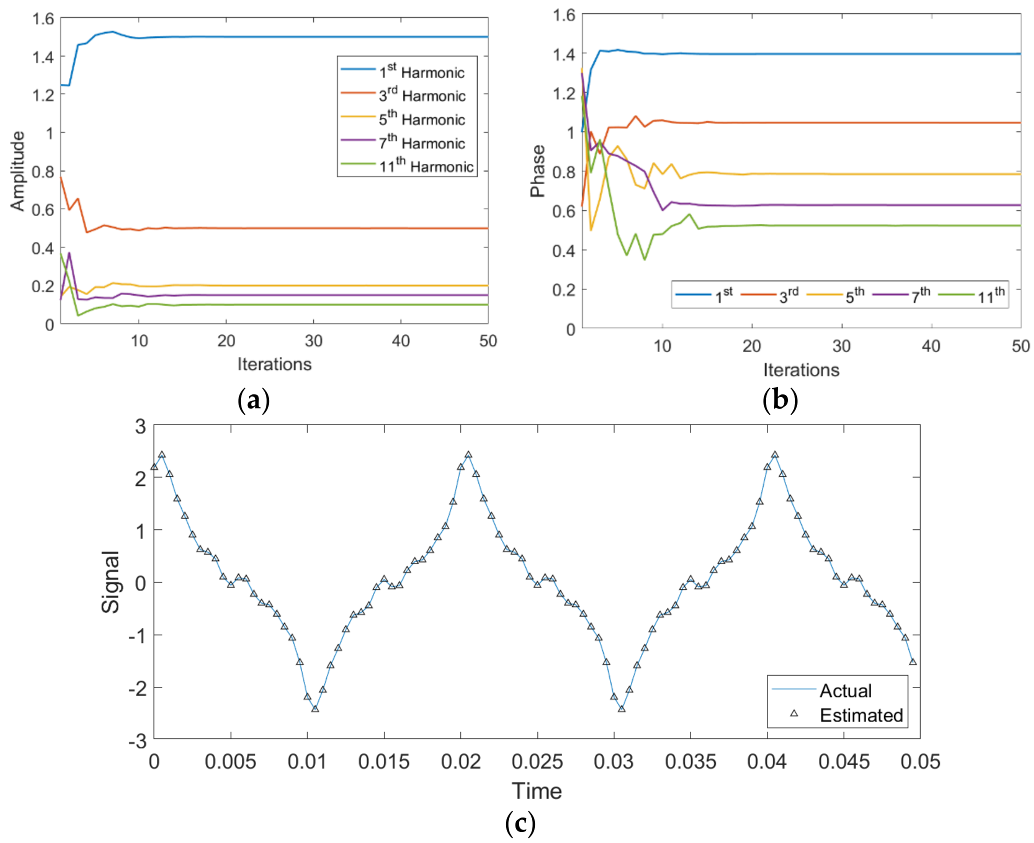

Figure 5. Plots of parameters estimates for 0.1 λ and 70 dB δ. (**a**) amplitude (**b**) phase (**c**) curve-fitting.

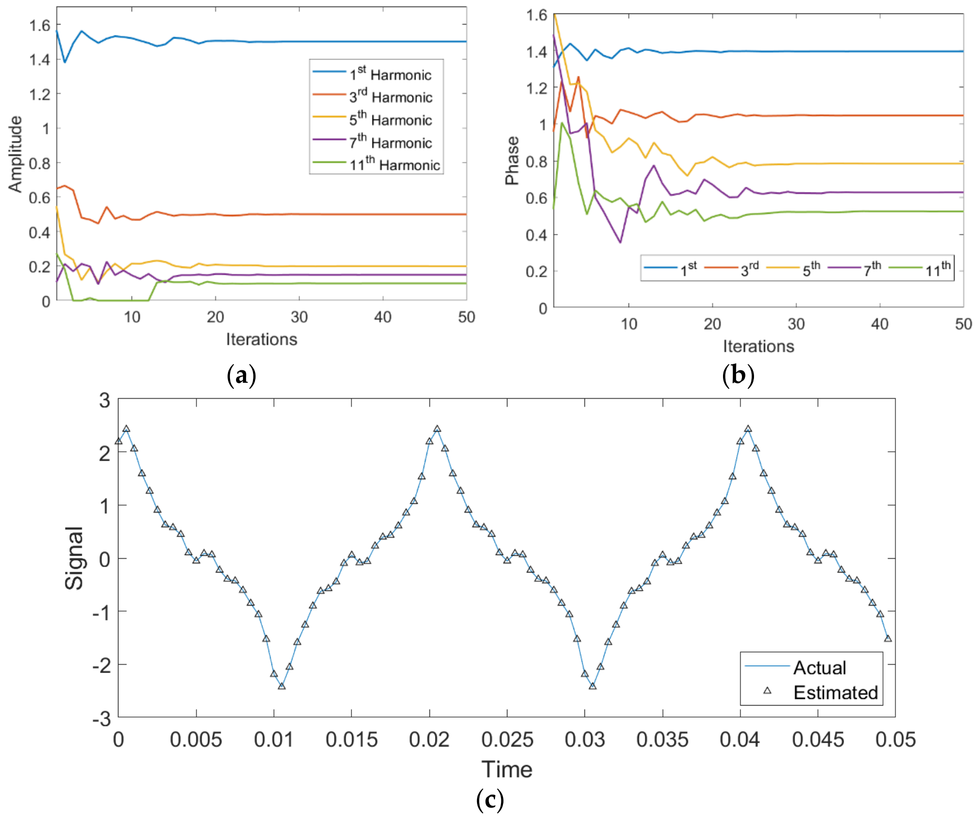

Figure 6. Plots of parameters estimates for 0.4 λ and 70 dB δ. (**a**) amplitude (**b**) phase (**c**) curve-fitting.

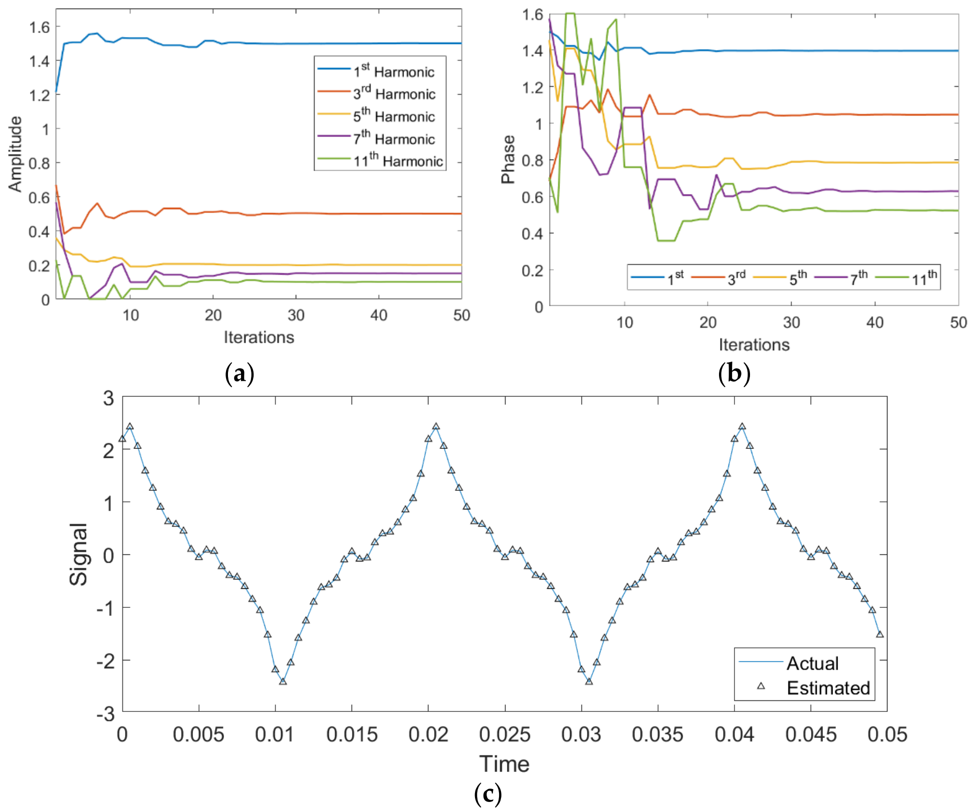

Figure 7. Plots of parameters estimate for 0.7 λ and 70 dB δ. (**a**) amplitude (**b**) phase (**c**) curve-fitting.

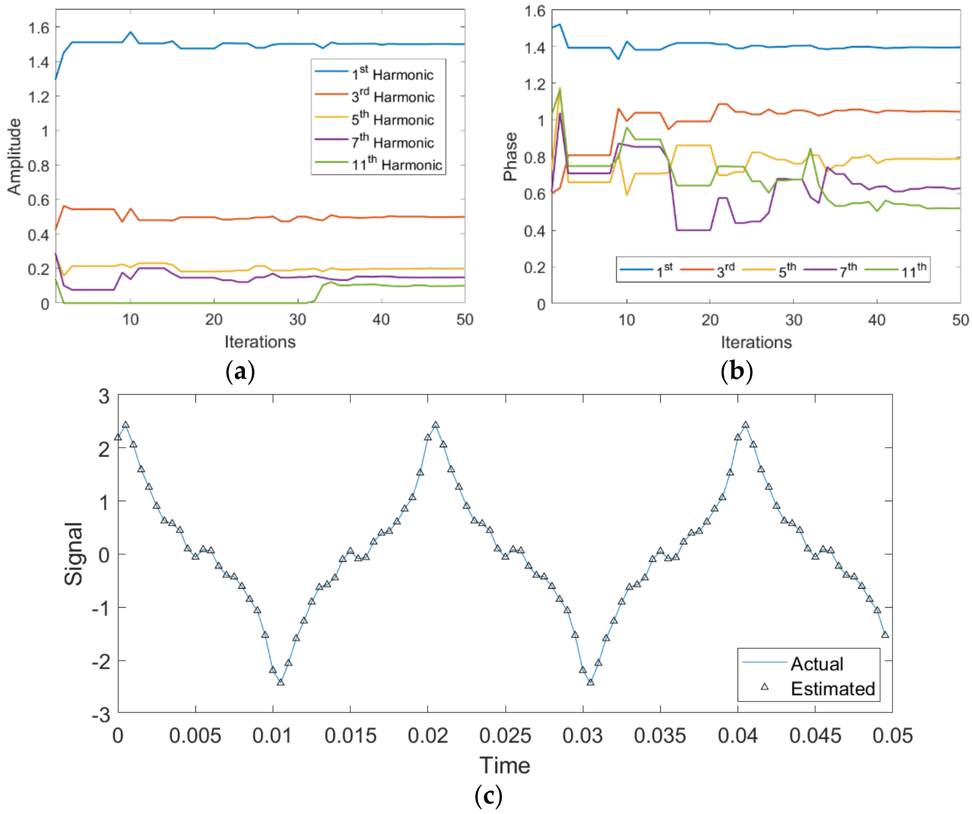

Figure 8. Plots of parameters estimates for 1.0 λ and 70 dB δ. (**a**) amplitude (**b**) phase (**c**) curve-fitting.

Furthermore, the reliability of the FOPSO was investigated through 50 autonomous executions; the results are presented in Figures 9–11 for λ = 0.1, 0.5 and 1.0, respectively. Figures 9a, 10a and 11a present the plots for δ = 200 dB, while Figures 9b, 10b and 11b present the plots for δ = 70 dB. Figures 9c, 10c and 11c present the plots for δ = 50 dB. The results indicated that the proposed FOPSO was more reliable for λ = 0.1, with almost the same trend in independent trials of the scheme, while for the case of standard PSO (FOPSO for λ = 1.0), variation in the results was observed, i.e., sometimes giving good results and sometimes not, as shown in Figure 11.

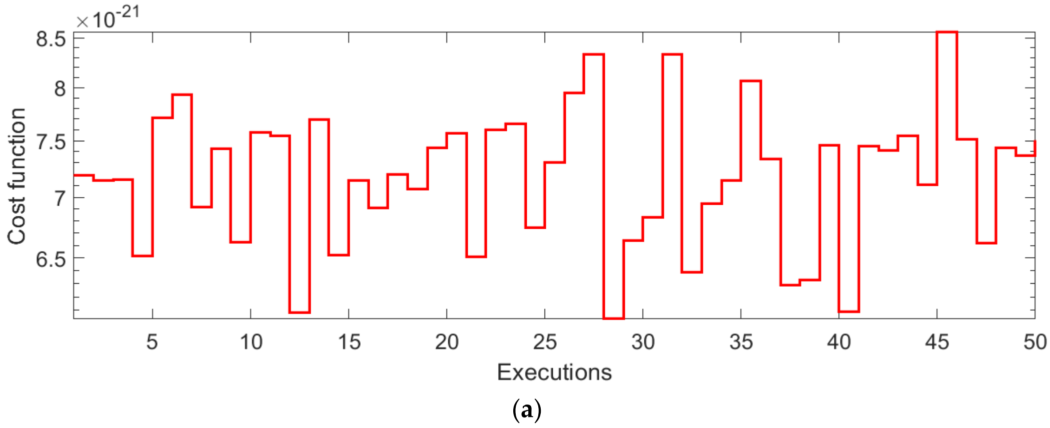

Figure 9. *Cont.*

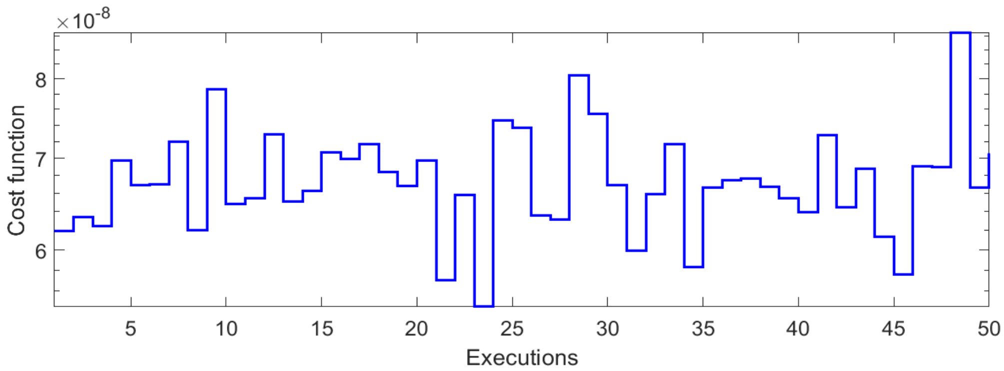

(**b**)

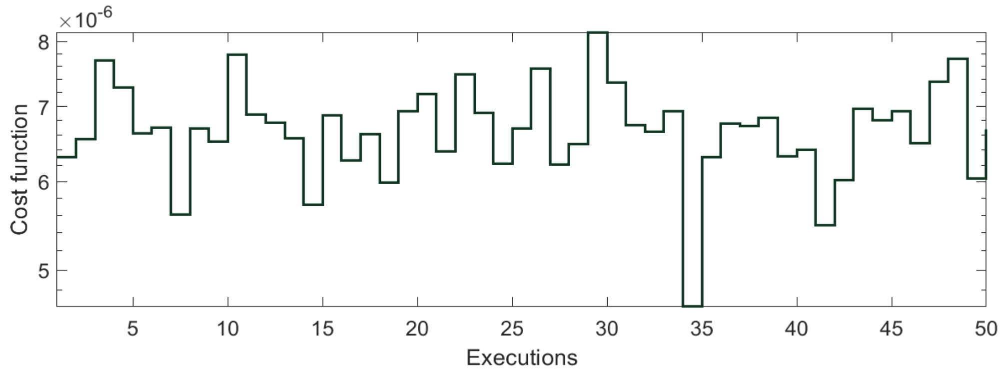

(**c**)

Figure 9. Monte Carlo simulation results for 0.1 λ (**a**) 200 dB (**b**) 70 dB (**c**) 50 dB.

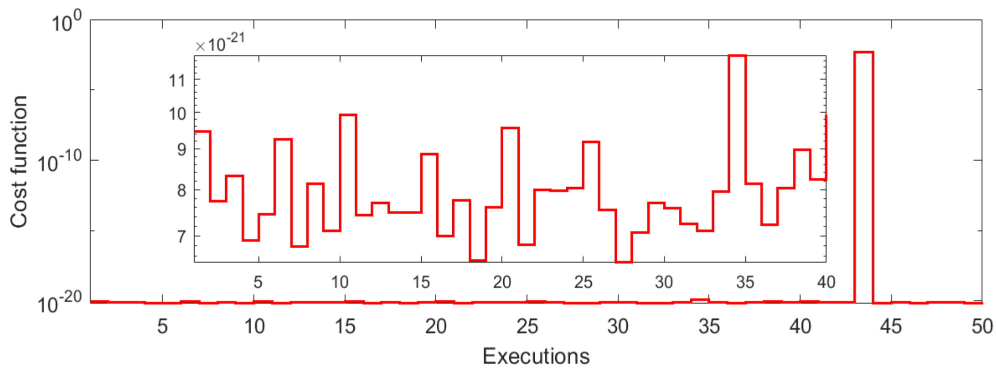

(**a**)

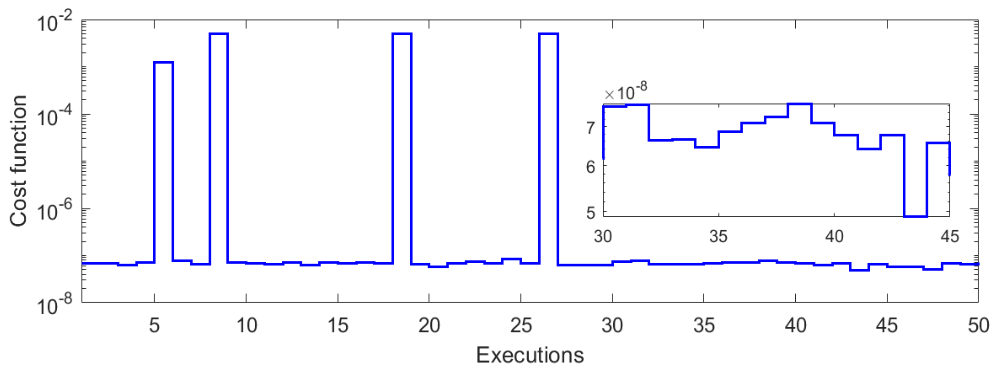

(**b**)

Figure 10. *Cont*.

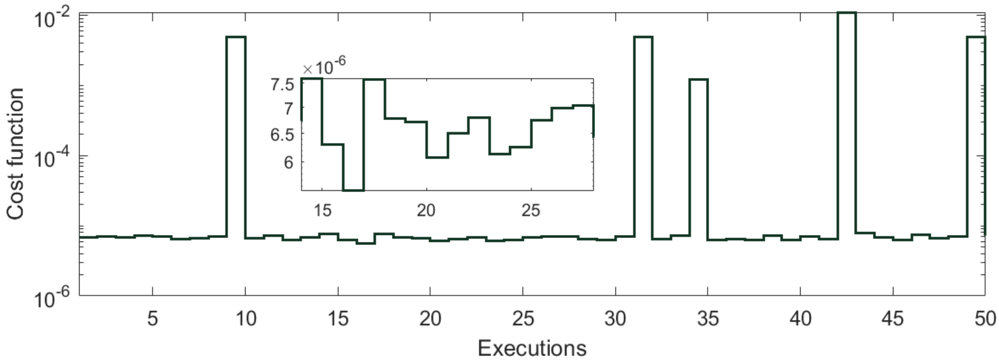

(**c**)

Figure 10. Monte Carlo simulation results for 0.5 λ (**a**) 200 dB (**b**) 70 dB (**c**) 50 dB.

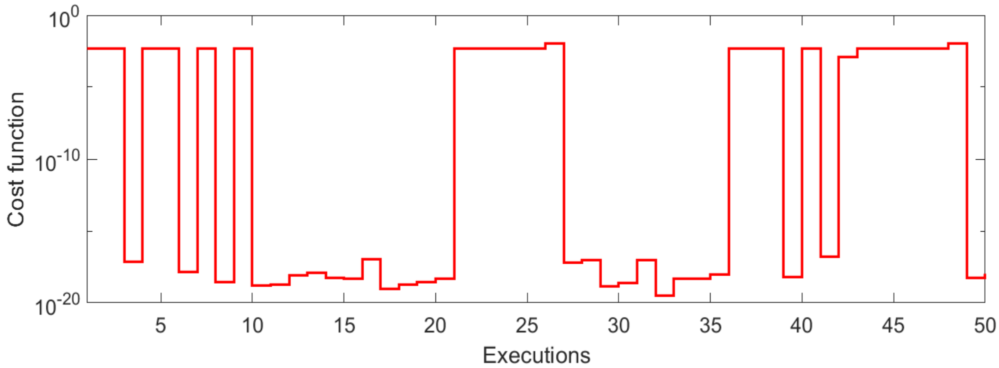

(**a**)

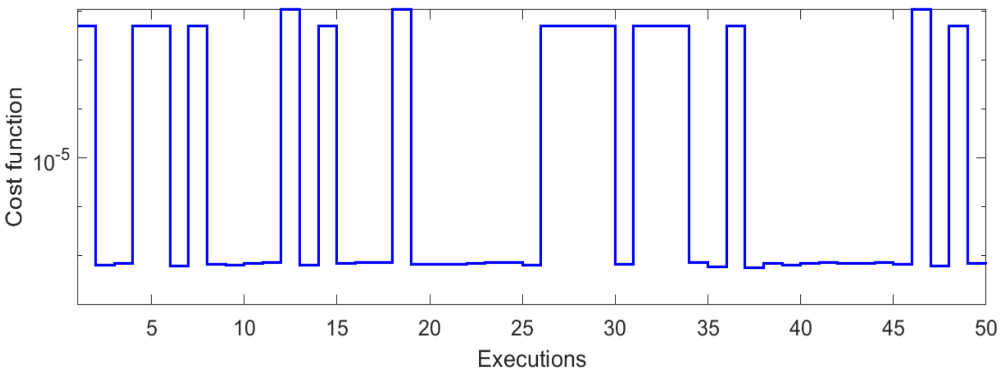

(**b**)

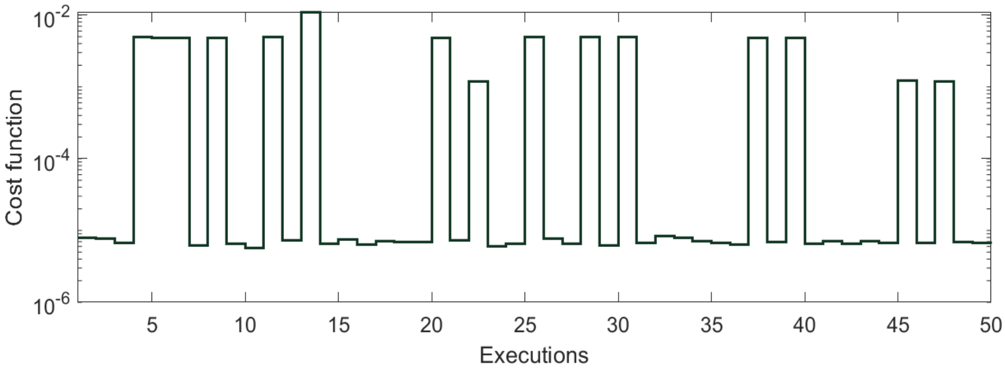

(**c**)

Figure 11. Monte Carlo simulation results for 1.0 λ (**a**) 200 dB (**b**) 70 dB (**c**) 50 dB.

Analyses in terms of statistical indices of the minimum (Mini) value of cost function, the mean and standard deviation (STDD) were conducted and the results are reported in Table 4. The Mini values indicated that the FOPSO was accurate and convergent for all λ and δ with decrease in the precision of the estimates as the noise δ increased. The small STDD values in the case of λ = 0.1 were 6.23×10^{-22}, 5.79×10^{-9} and 6.36×10^{-7} for δ = 200 dB, 70 dB and 50 dB, respectively, confirming the more reliable and consistently accurate behavior of the FOPSO for λ = 0.1. While the respective STDD values in the case of λ = 0.5 and λ = 1.0 were 7.07×10^{-4}, 1.20×10^{-3} and 1.92×10^{-3}, and 3.03×10^{-3}, 3.23×10^{-3} and 2.45×10^{-3}, respectively.

Table 4. Values of statistical indices through Monte Carlo simulations.

	δ = 200 dB			δ = 70 dB			δ = 50 dB		
λ	**Mini**	**Mean**	**STDD**	**Mini**	**Mean**	**STDD**	**Mini**	**Mean**	**STDD**
0.1	6.03×10^{-21}	7.24×10^{-21}	6.23×10^{-22}	5.45×10^{-8}	6.75×10^{-8}	5.79×10^{-9}	4.64×10^{-6}	6.69×10^{-6}	6.36×10^{-7}
0.2	5.39×10^{-21}	1.00×10^{-4}	7.07×10^{-4}	5.46×10^{-8}	4.24×10^{-4}	1.85×10^{-3}	5.80×10^{-6}	1.04×10^{-4}	6.86×10^{-4}
0.3	6.23×10^{-21}	3.00×10^{-4}	1.20×10^{-3}	5.38×10^{-8}	2.99×10^{-4}	1.20×10^{-3}	5.31×10^{-6}	6.62×10^{-6}	5.76×10^{-7}
0.4	5.66×10^{-21}	6.00×10^{-4}	1.64×10^{-3}	5.17×10^{-8}	5.98×10^{-4}	1.64×10^{-3}	5.51×10^{-6}	8.11×10^{-4}	2.17×10^{-3}
0.5	6.48×10^{-21}	1.00×10^{-4}	7.07×10^{-4}	4.89×10^{-8}	3.24×10^{-4}	1.20×10^{-3}	5.52×10^{-6}	5.43×10^{-4}	1.92×10^{-3}
0.6	6.47×10^{-21}	9.00×10^{-4}	1.94×10^{-3}	5.96×10^{-8}	1.12×10^{-3}	2.42×10^{-3}	5.71×10^{-6}	1.23×10^{-3}	2.71×10^{-3}
0.7	7.08×10^{-21}	1.02×10^{-3}	2.36×10^{-3}	5.84×10^{-8}	7.23×10^{-4}	1.75×10^{-3}	5.82×10^{-6}	1.05×10^{-3}	2.30×10^{-3}
0.8	8.51×10^{-21}	1.42×10^{-3}	2.58×10^{-3}	5.89×10^{-8}	1.72×10^{-3}	3.14×10^{-3}	5.18×10^{-6}	1.52×10^{-3}	2.55×10^{-3}
0.9	1.52×10^{-20}	2.13×10^{-3}	3.19×10^{-3}	5.69×10^{-8}	2.37×10^{-3}	3.65×10^{-3}	5.45×10^{-6}	1.93×10^{-3}	2.91×10^{-3}
1.0	9.89×10^{-20}	2.47×10^{-3}	3.03×10^{-3}	5.63×10^{-8}	2.07×10^{-3}	3.23×10^{-3}	5.62×10^{-6}	1.37×10^{-3}	2.45×10^{-3}

5. Conclusions

The findings/conclusions of the study are presented below.

A fractional order particle swarm optimization, FOPSO, was presented for solving nonlinear problems of harmonics estimation required for monitoring power quality in electrical systems to avoid any adverse effect of harmonic pollution. The FOPSO integrates the inherited legacy of fractional calculus with standard PSO to enhance its optimization capabilities with more controlling parameters. The FOPSO effectively estimated the amplitude and phase parameters of the harmonic signal compared with the standard counterpart for different scenarios of additive white Gaussian noise.

The FOPSO provided faster convergence speeds for a lower value of fractional order, i.e., 0.1 λ; and the convergence speed decreased gradually with increase in the fractional order, i.e., 0.1 λ to 1.0 λ. The FOPSO was robust against different levels of additive white Gaussian noise with relatively low estimation accuracy for high noise levels. The estimation errors for 200 db, 70 db and 50 db were approximately 10^{-21}, 10^{-8} and 10^{-6}, respectively. The statistical indices obtained through Monte Carlo simulations confirmed that the FOPSO was accurate and robust for all λ values in terms of best fitness, while, in terms of mean fitness values, the FOPSO with 0.1 λ was the best among all other fractional order variations.

In future, the proposed scheme can be exploited to solve different control and estimation problems [51–54]. Moreover, investigations can be carried out in implementing proposed schemes to solve the challenges involved in current power systems, such as, estimating the components that are not integer multiples of the fundamental harmonic, fault detection in power systems and machines, and estimating the exact frequency of the fundamental in real time.

Supplementary Materials: The following supporting information can be downloaded at: https://www.mdpi.com/article/10.3390/math10091570/s1: The parameter estimates results for remaining fractional orders, λ = 0.2, 0.3, 0.4, 0.6, 0.7, 0.8 and 0.9, are provided in Supplementary Tables S1–S7. The learning plots of amplitude and phase parameters estimates, along with the constructed harmonic signal from the estimated parameters, are presented in Supplementary Figures S1–S4 for λ = 0.1, 0.4, 0.7 and 1.0, respectively, in the case of δ = 2000 dB, while the respective plots for 50 dB are provided in Supplementary Figures S5–S8, respectively.

Author Contributions: Conceptualization, N.I.C. and M.A.Z.R.; methodology, N.A.M., N.I.C. and M.A.Z.R.; software, N.A.M.; validation, M.A.Z.R. and N.I.C.; resources, C.-L.C. and C.-M.S.; writing—original draft preparation, N.A.M.; writing—review and editing, N.I.C. and M.A.Z.R.; supervision, C.-L.C.; project administration, K.M.C., C.-M.S. and S.S.A.; funding acquisition, K.M.C. and S.S.A. All authors have read and agreed to the published version of the manuscript.

Funding: Taif University Researchers supporting Project number (TURSP-2020/215), Taif University, Taif, Saudi Arabia.

Conflicts of Interest: The authors declare no conflict of interest.

References

1. Van Der Heijden, F.; Duin, R.P.; De Ridder, D.; Tax, D.M. *Classification, Parameter Estimation and State Estimation: An Engineering Approach Using MATLAB*; John Wiley & Sons: Hoboken, NJ, USA, 2005.
2. Silvey, S. *Optimal Design: An Introduction to the Theory for Parameter Estimation*; Springer Science & Business Media: Berlin, Germany, 2013; Volume 1.
3. Mehmood, A.; Zameer, A.; Chaudhary, N.I.; Ling, S.H.; Raja, M.A.Z. Design of meta-heuristic computing paradigms for Hammerstein identification systems in electrically stimulated muscle models. *Neural Comput. Appl.* **2020**, *32*, 12469–12497. [CrossRef]
4. Raja, M.A.Z.; Shah, A.A.; Mehmood, A.; Chaudhary, N.I.; Aslam, M.S. Bio-inspired computational heuristics for parameter estimation of nonlinear Hammerstein controlled autoregressive system. *Neural Comput. Appl.* **2018**, *29*, 1455–1474. [CrossRef]
5. Yang, X.; Yang, Y.; Liu, Y.; Deng, Z. A reliability assessment approach for electric power systems considering wind power uncertainty. *IEEE Access* **2020**, *8*, 12467–12478. [CrossRef]
6. Beleiu, H.G.; Maier, V.; Pavel, S.G.; Birou, I.; Pică, C.S.; Dărab, P.C. Harmonics consequences on drive systems with induction motor. *Appl. Sci.* **2020**, *10*, 1528. [CrossRef]
7. Almutairi, M.S.; Hadjiloucas, S. Harmonics mitigation based on the minimization of non-linearity current in a power system. *Designs* **2019**, *3*, 29. [CrossRef]
8. Phannil, N.; Jettanasen, C.; Ngaopitakkul, A. Harmonics and reduction of energy consumption in lighting systems by using LED lamps. *Energies* **2018**, *11*, 3169. [CrossRef]
9. Singh, S.K.; Sinha, N.; Goswami, A.K.; Sinha, N. Several variants of Kalman Filter algorithm for power system harmonic estimation. *Int. J. Electr. Power Energy Syst.* **2016**, *78*, 793–800. [CrossRef]
10. Joorabian, M.; Mortazavi, S.S.; Khayyami, A.A. Harmonic estimation in a power system using a novel hybrid Least Squares-Adaline algorithm. *Electr. Power Syst. Res.* **2009**, *79*, 107–116. [CrossRef]
11. Enayati, J.; Moravej, Z. Real-time harmonics estimation in power systems using a novel hybrid algorithm. *IET Gener. Transm. Distrib.* **2017**, *11*, 3532–3538. [CrossRef]
12. Sarkar, A.; Choudhury, S.R.; Sengupta, S. A self-synchronized ADALINE network for on-line tracking of power system harmonics. *Measurement* **2011**, *44*, 784–790. [CrossRef]
13. Liu, S.; Ding, F.; Xu, L.; Hayat, T. Hierarchical principle-based iterative parameter estimation algorithm for dual-frequency signals. *Circuits Syst. Signal Process.* **2019**, *38*, 3251–3268. [CrossRef]
14. Xu, L.; Chen, F.; Ding, F.; Alsaedi, A.; Hayat, T. Hierarchical recursive signal modeling for multifrequency signals based on discrete measured data. *Int. J. Adapt. Control Signal Process.* **2021**, *35*, 676–693. [CrossRef]
15. Xu, L.; Ding, F.; Zhu, Q. Separable synchronous multi-innovation gradient-based iterative signal modeling from on-line measurements. *IEEE Trans. Instrum. Meas.* **2022**, *71*, 6501313. [CrossRef]
16. Mirjalili, S.; Faris, H.; Aljarah, I. *Evolutionary Machine Learning Techniques*; Springer: Singapore, 2019.
17. Mohammadian, M.; Lorestani, A.; Ardehali, M.M. Optimization of single and multi-areas economic dispatch problems based on evolutionary particle swarm optimization algorithm. *Energy* **2018**, *161*, 710–724. [CrossRef]
18. Mehmood, A.; Raja, M.A.Z.; Shi, P.; Chaudhary, N.I. Weighted differential evolution-based heuristic computing for identification of Hammerstein systems in electrically stimulated muscle modeling. *Soft Comput.* **2022**, 1–17. [CrossRef]
19. Ray, P.K.; Subudhi, B. BFO optimized RLS algorithm for power system harmonics estimation. *Appl. Soft Comput.* **2012**, *12*, 1965–1977. [CrossRef]
20. Mehmood, A.; Chaudhary, N.I.; Raja, M.A.Z. Novel computing paradigms for parameter estimation in power signal models. *Neural Comput. Appl.* **2020**, *32*, 6253–6282. [CrossRef]
21. Mehmood, A.; Shi, P.; Raja, M.A.Z.; Zameer, A.; Chaudhary, N.I. Design of backtracking search heuristics for parameter estimation of power signals. *Neural Comput. Appl.* **2021**, *33*, 1479–1496. [CrossRef]
22. Elvira-Ortiz, D.A.; Jaen-Cuellar, A.Y.; Morinigo-Sotelo, D.; Morales-Velazquez, L.; Osornio-Rios, R.A.; Romero-Troncoso, R.d.J. Genetic algorithm methodology for the estimation of generated power and harmonic content in photovoltaic generation. *Appl. Sci.* **2020**, *10*, 542. [CrossRef]
23. do Nascimento Sepulchro, W.; Encarnação, L.F.; Brunoro, M. Harmonic state and power flow estimation in distribution systems using evolutionary strategy. *J. Control Autom. Electr. Syst.* **2014**, *25*, 358–367. [CrossRef]

24. Subramaniyan, S.; Ramiah, J. Improved football game optimization for state estimation and power quality enhancement. *Comput. Electr. Eng.* **2020**, *81*, 106547. [CrossRef]
25. Singh, S.K.; Sinha, N.; Goswami, A.K.; Sinha, N. Robust estimation of power system harmonics using a hybrid firefly based recursive least square algorithm. *Int. J. Electr. Power Energy Syst.* **2016**, *80*, 287–296. [CrossRef]
26. Kabalci, Y.; Kockanat, S.; Kabalci, E. A modified ABC algorithm approach for power system harmonic estimation problems. *Electr. Power Syst. Res.* **2018**, *154*, 160–173. [CrossRef]
27. Yu, Z.; Sun, G.; Lv, J. A fractional-order momentum optimization approach of deep neural networks. *Neural Comput. Appl.* **2022**, *34*, 7091–7111. [CrossRef]
28. Chaudhary, N.I.; Raja, M.A.Z.; Khan, Z.A.; Mehmood, A.; Shah, S.M. Design of fractional hierarchical gradient descent algorithm for parameter estimation of nonlinear control autoregressive systems. *Chaos Solitons Fractals* **2022**, *157*, 111913. [CrossRef]
29. Machado, J.T.; Kiryakova, V.; Mainardi, F. Recent history of fractional calculus. *Commun. Nonlinear Sci. Numer. Simul.* **2011**, *16*, 1140–1153. [CrossRef]
30. Akdemir, A.O.; Butt, S.I.; Nadeem, M.; Ragusa, M.A. New general variants of Chebyshev type inequalities via generalized fractional integral operators. *Mathematics* **2021**, *9*, 122. [CrossRef]
31. Liu, X.; Bo, Y.; Jin, Y. A Numerical Method for the Variable-Order Time-Fractional Wave Equations Based on the H2N2 Approximation. *J. Funct. Spaces* **2022**, *2022*, 3438289. [CrossRef]
32. Khan, Z.A.; Chaudhary, N.I.; Zubair, S. Fractional stochastic gradient descent for recommender systems. *Electron. Mark.* **2019**, *29*, 275–285. [CrossRef]
33. Khan, Z.A.; Zubair, S.; Chaudhary, N.I.; Raja, M.A.Z.; Khan, F.A.; Dedovic, N. Design of normalized fractional SGD computing paradigm for recommender systems. *Neural Comput. Appl.* **2020**, *32*, 10245–10262. [CrossRef]
34. Yousri, D.; Mirjalili, S. Fractional-order cuckoo search algorithm for parameter identification of the fractional-order chaotic, chaotic with noise and hyper-chaotic financial systems. *Eng. Appl. Artif. Intell.* **2020**, *92*, 103662. [CrossRef]
35. Yousri, D.; Abd Elaziz, M.; Mirjalili, S. Fractional-order calculus-based flower pollination algorithm with local search for global optimization and image segmentation. *Knowl.-Based Syst.* **2020**, *197*, 105889. [CrossRef]
36. Yousri, D.; Mirjalili, S.; Machado, J.T.; Thanikanti, S.B.; Fathy, A. Efficient fractional-order modified Harris Hawks optimizer for proton exchange membrane fuel cell modeling. *Eng. Appl. Artif. Intell.* **2021**, *100*, 104193. [CrossRef]
37. Chaudhary, N.I.; Zubair, S.; Raja, M.A.Z. A new computing approach for power signal modeling using fractional adaptive algorithms. *ISA Trans.* **2017**, *68*, 189–202. [CrossRef] [PubMed]
38. Zubair, S.; Chaudhary, N.I.; Khan, Z.A.; Wang, W. Momentum fractional LMS for power signal parameter estimation. *Signal Process.* **2018**, *142*, 441–449. [CrossRef]
39. Chaudhary, N.I.; Latif, R.; Raja, M.A.Z.; Machado, J.T. An innovative fractional order LMS algorithm for power signal parameter estimation. *Appl. Math. Model.* **2020**, *83*, 703–718. [CrossRef]
40. Pires, E.J.S.; Machado, J.A.T.; Oliveira, P.B.M.; Cunha, J.B.; Mendes, L. Particle swarm optimization with fractional-order velocity. *Nonlinear Dyn.* **2010**, *61*, 295–301. [CrossRef]
41. Couceiro, M.S.; Rocha, R.P.; Ferreira, N.M.; Machado, J.A. Introducing the fractional-order Darwinian PSO. *Signal Image Video Process.* **2012**, *6*, 343–350. [CrossRef]
42. Ghamisi, P.; Couceiro, M.S.; Martins, F.M.; Benediktsson, J.A. Multilevel image segmentation based on fractional-order Darwinian particle swarm optimization. *IEEE Trans. Geosci. Remote Sens.* **2013**, *52*, 2382–2394. [CrossRef]
43. Shahri, E.S.A.; Alfi, A.; Machado, J.T. Fractional fixed-structure H∞ controller design using augmented Lagrangian particle swarm optimization with fractional order velocity. *Appl. Soft Comput.* **2019**, *77*, 688–695. [CrossRef]
44. Pahnehkolaei, S.M.A.; Alfi, A.; Machado, J.T. Analytical stability analysis of the fractional-order particle swarm optimization algorithm. *Chaos Solitons Fractals* **2022**, *155*, 111658. [CrossRef]
45. Zameer, A.; Muneeb, M.; Mirza, S.M.; Raja, M.A.Z. Fractional-order particle swarm based multi-objective PWR core loading pattern optimization. *Ann. Nucl. Energy* **2020**, *135*, 106982. [CrossRef]
46. Khan, M.W.; Muhammad, Y.; Raja, M.A.Z.; Ullah, F.; Chaudhary, N.I.; He, Y. A new fractional particle swarm optimization with entropy diversity based velocity for reactive power planning. *Entropy* **2020**, *22*, 1112. [CrossRef]
47. Muhammad, Y.; Khan, R.; Raja, M.A.Z.; Ullah, F.; Chaudhary, N.I.; He, Y. Design of fractional swarm intelligent computing with entropy evolution for optimal power flow problems. *IEEE Access* **2020**, *8*, 111401–111419. [CrossRef]
48. Sabatier, J.A.T.M.J.; Agrawal, O.P.; Machado, J.T. *Advances in Fractional Calculus*; Springer: Dordrecht, The Netherlands, 2007; Volume 4, p. 9.
49. Teodoro, G.S.; Machado, J.T.; De Oliveira, E.C. A review of definitions of fractional derivatives and other operators. *J. Comput. Phys.* **2019**, *388*, 195–208. [CrossRef]
50. Couceiro, M.; Ghamisi, P. *Fractional Order Darwinian Particle Swarm Optimization Applications and Evaluation of An Evolutionary Algorithm*; Springer: Berlin, Germany, 2016; ISBN 978-3-319-19634-3.
51. Chen, J.; Ma, J.; Gan, M.; Zhu, Q. Multi-direction gradient iterative algorithm: A unified framework for gradient iterative and least squares algorithms. *IEEE Trans. Autom. Control* **2021**. [CrossRef]

52. Chen, J.; Ding, F.; Zhu, Q.; Liu, Y. Interval error correction auxiliary model based gradient iterative algorithms for multirate ARX models. *IEEE Trans. Autom. Control* **2019**, *65*, 4385–4392. [CrossRef]
53. Xu, L.; Ding, F.; Yang, E. Auxiliary model multiinnovation stochastic gradient parameter estimation methods for nonlinear sandwich systems. *Int. J. Robust Nonlinear Control* **2021**, *31*, 148–165. [CrossRef]
54. Xu, L.; Ding, F.; Zhu, Q. Decomposition strategy-based hierarchical least mean square algorithm for control systems from the impulse responses. *Int. J. Syst. Sci.* **2021**, *52*, 1806–1821. [CrossRef]